


 Cite this: *Nanoscale*, 2017, **9**, 9902

Insulated molecular wires: inhibiting orthogonal contacts in metal complex based molecular junctions†

Oday A. Al-Owaedi,^{‡,a,b} Sören Bock,^{‡,c} David C. Milan,^{‡,d} Marie-Christine Oerthel,^e Michael S. Inkpen,^{‡,f} Dmitry S. Yufit,^{‡,g} Alexandre N. Sobolev,^{c,g} Nicholas J. Long,^{‡,f} Tim Albrecht,^{‡,f} Simon J. Higgins,^{‡,d} Martin R. Bryce,^{‡,e} Richard J. Nichols,^{‡,d} Colin J. Lambert,^{‡,a} and Paul J. Low,^{‡,c}

Metal complexes are receiving increased attention as molecular wires in fundamental studies of the transport properties of metal|molecule|metal junctions. In this context we report the single-molecule conductance of a systematic series of d^8 square-planar platinum(II) *trans*-bis(alkynyl) complexes with terminal trimethylsilylethynyl ($C\equiv CSiMe_3$) contacting groups, *e.g.* *trans*-Pt($C\equiv CC_6H_4C\equiv CSiMe_3$)₂(PR₃)₂ (R = Ph or Et), using a combination of scanning tunneling microscopy (STM) experiments in solution and theoretical calculations using density functional theory and non-equilibrium Green's function formalism. The measured conductance values of the complexes (*ca.* $3\text{--}5 \times 10^{-5} G_0$) are commensurate with similarly structured all-organic oligo(phenylene ethynylene) and oligo(yne) compounds. Based on conductance and break-off distance data, we demonstrate that a PPh₃ supporting ligand in the platinum complexes can provide an alternative contact point for the STM tip in the molecular junctions, orthogonal to the terminal $C\equiv CSiMe_3$ group. The attachment of hexyloxy side chains to the diethynylbenzene ligands, *e.g.* *trans*-Pt($C\equiv CC_6H_2(Ohex)_2C\equiv CSiMe_3$)₂(PPh₃)₂ (Ohex = OC₆H₁₃), hinders contact of the STM tip to the PPh₃ groups and effectively insulates the molecule, allowing the conductance through the full length of the backbone to be reliably measured. The use of trialkylphosphine (PEt₃), rather than triarylphosphine (PPh₃), ancillary ligands at platinum also eliminates these orthogonal contacts. These results have significant implications for the future design of organometallic complexes for studies in molecular junctions.

Received 15th March 2017,
Accepted 25th June 2017

DOI: 10.1039/c7nr01829k
rsc.li/nanoscale

^aDepartment of Physics, University of Lancaster, Lancaster, LA1 4YB, UK.

E-mail: paul.low@uwa.edu.au

^bDepartment of Laser Physics, Women Faculty of Science, Babylon University, Hilla, Iraq

^cSchool of Molecular Sciences, University of Western Australia, 35 Stirling Highway, Perth 6009, Australia

^dDepartment of Chemistry, University of Liverpool, Crown St, Liverpool, L69 7ZD, UK

^eDepartment of Chemistry, Durham University, South Rd, Durham, DH1 3LE, UK

^fDepartment of Chemistry, Imperial College London, London SW7 2AZ, UK

^gCentre for Microscopy Characterization and Analysis, University of Western Australia, 35 Stirling Highway, Perth 6009, Australia

† Electronic supplementary information (ESI) available: Synthetic procedures and characterisation data. Details of computational analysis, descriptions of alternate junction geometries, plots showing calculated conductance as a function of Fermi energy for these different models and tabulated results. Plots of NMR spectra. Data from the single molecule studies is available from the University of Liverpool data catalogue (DOI: 10.17638/datacat.liverpool.ac.uk/212). See DOI: 10.1039/c7nr01829k

‡ These authors contributed equally.

Introduction

The development of methods that allow the formation and experimental determination of the electrical response of single-molecule metal|molecule|metal junctions has driven rapid advances in molecular electronics.^{1–6} Studies of simple systems such as α,ω -alkane dithiols contacted between two gold electrodes have shed light on issues such as non-resonant charge transport and the importance of molecular conformation within the junction,^{7–9} and inspired innovations in designs of wire-like molecules. Moving beyond the identification of the influence of the medium on electrical properties of the junction^{10–14} and introduction of redox-active molecules to molecular junctions has led to systems capable of modulating charge transport in response to an external electrochemical or chemical gate.^{15–20}

Whilst the majority of studies have been directed towards organic molecules within molecular junctions, metal complexes are now also attracting attention.^{21–24} Metal complexes offer the potential to tune energies of key molecular orbitals



through choice of metal and supporting ligands, whilst the possibilities to control the metal complex redox state at modest potentials leads to exciting applications in electrostatically and electrochemically gated junctions.^{25,26} Of the various metal complexes that have been studied in molecular junctions, including multi-metallic strings,²⁷ clusters,^{13,28,29} porphyrins,^{30,31} and ferrocene derivatives,^{32,33} compounds and complexes of the group 8 metals within bipyridyl-,^{34–36} bis(terpyridyl)-³⁷ or *trans*-bis(alkynyl)-based^{38,39,40–46} structures feature prominently. In contrast, analogous wire-like *trans*-bis(alkynyl) platinum complexes have been little explored in molecular junctions.^{47–49} This is likely due to the perceptions of low conductivity arising from the smaller contribution of Pt (5d) orbitals to the frontier orbitals of square planar *trans*-Pt(C≡CR)₂L₂ (L = phosphine) complexes compared with the more extensive delocalisation in the HOMOs of octahedral complexes *trans*-M(C≡CR)₂L₄ (M = Fe, Ru, Os) along the π-d-π-conjugated molecular backbone.^{45,50–53} However, as discussed by McGrady in the context of pseudo-1D metal string complexes, efficient through-molecule conductance can be achieved through frontier orbitals which are distributed near, and energetically aligned with, the electrodes and need not be evenly distributed along the entire molecular backbone.^{54,55} Recently, the molecular conductances of Pt(II) complexes *trans*-Pt{C≡CC₆H₂(Ohex)₂C≡CC₆H₄SM₂}₂(PPh₃)₂ (1.8 × 10^{−5} G₀) and *trans*-Pt{C≡CC₆H₂(Ohex)₂C≡CC₅H₄N}₂(PPh₃)₂ (9.8 × 10^{−6} G₀) have been measured, and found to be similar to those of analogous ruthenium complexes *trans*-Ru{C≡CC₆H₂(Ohex)₂C≡CC₆H₄SM₂}₂(dppe)₂ (1.8 × 10^{−5} G₀) and *trans*-Ru{C≡CC₆H₂(Ohex)₂C≡CC₅H₄N}₂(dppe)₂ (4.5 × 10^{−6} G₀),⁵⁶ (Ohex = OC₆H₁₃) making *trans*-bis(alkynyl) Pt(II) complexes an attractive target for further study.

Through numerous studies of molecular junctions, the nature of the molecule-electrode contact has proven important,⁵⁷ and recognition of the role that anchor groups play in the electrical performance of the junction has led to the development of a wide range of contacting groups and electrode materials.^{58–63} However, even well-known contacting groups such as thiolates bind to a range of surface sites, including terraces or near to adatoms as well as idealised pristine atomically flat terraces, giving rise to a range of molecular conductance signatures from a given molecular backbone.⁶⁴ Consequently, interest has increasingly focussed on molecular junctions in which the molecule is contacted to the electrode by strong electrode-carbon covalent bonds.^{65,66} Other strategies to minimise the range of conductance signatures observed include the use of bulky anchor groups such as trimethylsilylthynyl, which give rise only to junctions of appreciable conductance in a restricted range of configurations, simplifying conductance profiles and allowing more precise assessment of low conductance contacts.^{14,67}

However, even when well-defined contacts are placed within a molecule, the contact of the electrodes to different parts of the compound, particularly in the case of long, conjugated molecules, can result in complex electrical behavior. Examples include the potentiometric-like response of thiol-terminated

oligoenes, where electrical contact can be made at either the thiol or oligoene π-system,⁶⁸ and related observations in oligoynes-based⁶⁹ and other molecular wires^{70,71} in which the π-system of the molecular backbone interacts with the electrodes at shorter electrode separations leading to enhanced conductance (short circuits).

Observations of electrical contact directly to the molecular backbone, and conceptual analogies to conventional wires, inspire the design of ‘insulated’ wire-like compounds.^{72,73} For example, the Gladysz group has reported a series of bimetallic, polyndiyi-bridged platinum complexes in which the wire-like polyndiyi core is wrapped in helical alkyl chains (Fig. 1a).^{74–79}

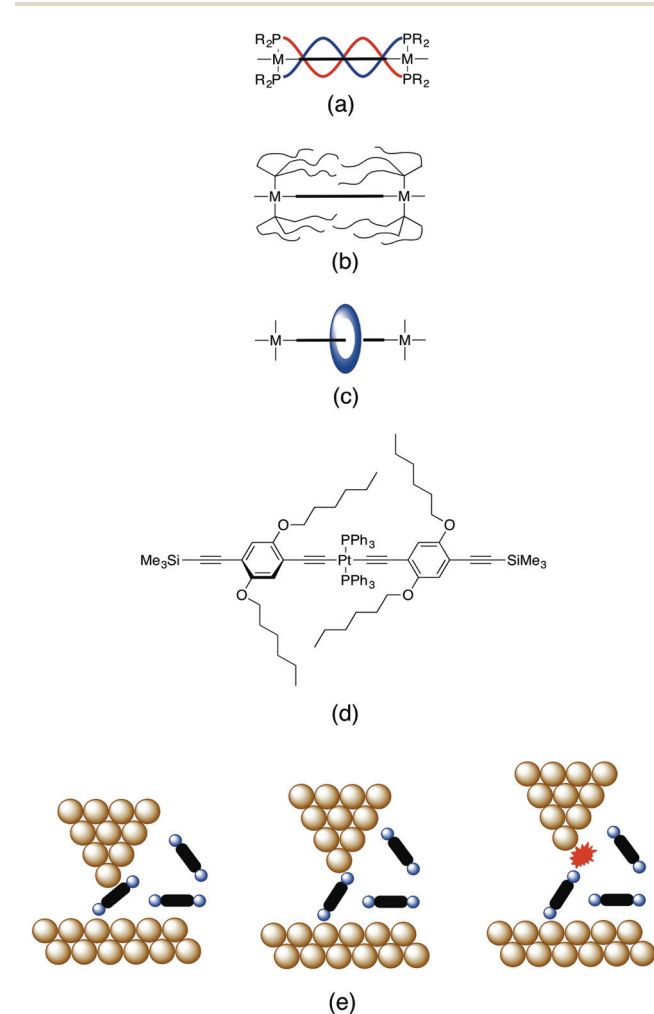


Fig. 1 Representative sketches of different insulating strategies for metal-complex based molecular wires: (a) helical alkyl chains arranged around a conjugated chain (bold line); (b) fluorous alkyl chains self-assembled around a conjugated chain; (c) encapsulation of a conjugated chain in a rotaxane-like structure; (d) protection of the ancillary ligands on the metal complex by alkyloxy side-chains; (e) single molecule conductance can be determined by placing the molecule within a junction represented here by an STM tip and a conducting substrate. After initial contact with the molecule, the current flowing from the tip to the substrate through the molecule is determined whilst the STM tip is withdrawn. As the tip is withdrawn the molecule may rearrange within the junction until eventually the tip|molecule|substrate contact is broken.¹



A related concept involving the introduction of highly fluorous trialkylphosphines as ancillary ligands to bimetallic platinum polyyndiyl complexes to shield the wire-like carbon-chain through aggregation of the fluorine-rich aliphatic segments has also been proposed (Fig. 1b).⁸⁰ Rotaxane-like encapsulation has also proven to be a popular concept in the design of insulated wire-like structures, with prominent recent examples from the Anderson and Tykwinski,^{81,82} Gladysz^{83,84} and Terao^{85–89} groups being reported recently (Fig. 1c). In each of these cases, the conceptual design principle involves shielding the π -conjugated backbone of the molecule from adventitious contact within a junction.⁹⁰

The motivation for the present study was twofold: (i) to explore the electrical properties and behavior of new *trans*-bis(alkynyl) platinum complexes within molecular junctions, and (ii) to address issues concerning the design of insulated molecular wires. We demonstrate that when contacted through the trimethylsilylethynyl group installed at the remote ends of the molecular backbone, the *trans*-bis(alkynyl) platinum complexes examined here display single molecule conductances of similar magnitude to organic oligo(phenylene ethynylene)- and oligo(yne)-based molecular wires. In addition, hexyloxy side chains, initially introduced to promote solubility (Fig. 1d), are shown to play an important role in preventing adventitious contacts ('short circuits') by hindering formation of molecular junctions contacted through ancillary triphenylphosphine (PPh_3) ligands.

Results and discussion

The compounds **1a,b–4a,b** (Chart 1) were chosen to allow further exploration of the behavior of *trans*-bis(alkynyl) Pt(n) complexes and the influence of supporting ligands in single-molecule junctions. The trimethylsilylethynyl group ($\text{C}\equiv\text{CSiMe}_3$) has been shown to be a useful anchor in the construction of self-assembled monolayers (SAMs) of unsaturated hydrocarbons on gold, with the electron-withdrawing ethynyl moiety playing an essential role in stabilizing the gold–molecule interaction.^{91–94} As a contacting group in molecular junctions, the $\text{C}\equiv\text{CSiMe}_3$ moiety is known to favor only a single, albeit low conductance, contact.^{14,95–97} This is due to the fact that the $\text{C}\equiv\text{CSiMe}_3$ group makes effective electrical contact to defect sites on the gold electrode surfaces in a restricted range of geometries, limited in part due to the steric bulk of the ancillary methyl groups.⁶⁷ Thus, in even π -rich oligophenylene ethynylene based molecules, the large footprint and limited range of conducting configurations that are available to $\text{C}\equiv\text{CSiMe}_3$ contacts gives rise to conductance histograms featuring only a single conductance peak without complications from alternative conductive molecular orientations or contacts within the junction^{14,14,67,96} As will be seen in the discussion that follows, the relatively weak nature of the $\text{C}\equiv\text{CSiMe}_3$ –gold interaction (estimated at *ca.* 0.4–0.7 eV)^{14,67} permits competitive, if adventitious, interactions between the STM tip and other regions of the molecule.

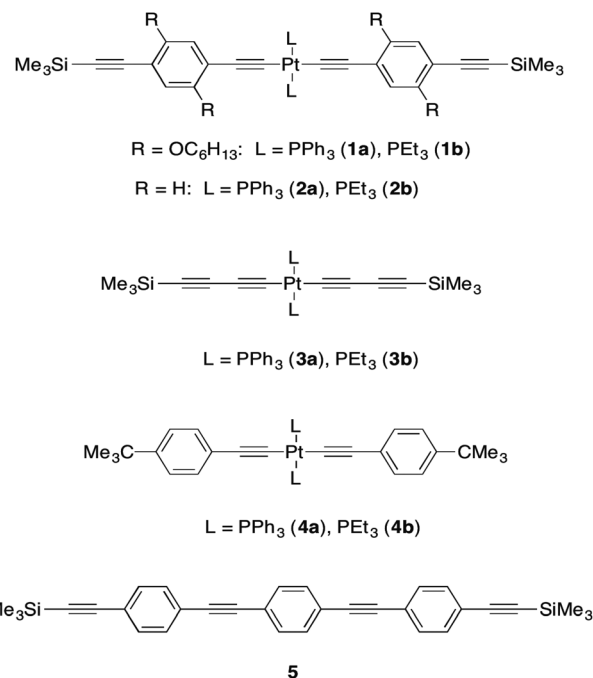


Chart 1 The compounds **1a,b–4a,b** used in this work, and reference compound **5**.

The complexes were synthesized from CuI-catalyzed ligand exchange reactions of *cis*- $\text{PtCl}_2(\text{PPh}_3)_2$ ⁹⁸ or a mixture of *cis*- and *trans*- $\text{PtCl}_2(\text{PEt}_3)_2$ ⁹⁹ with the appropriate alkyne in diethyl-, triethyl- or diisopropyl-amine solvent.¹⁰⁰ The compounds were characterized by the usual suite of ^1H , ^{13}C and ^{31}P NMR spectroscopies, IR spectroscopy, mass spectrometry, and elemental analysis. Complexes **2a** and **2b** were also characterized by single crystal X-ray diffraction studies, the results of which are summarized in the ESI.† Conductance data were acquired using the STM $I(s)$ technique (Fig. 1e and Fig. S1–S8†),¹⁰¹ with measurements made in mesitylene solution.¹⁴ These experimental measurements were also supported by calculations of model junctions carried out using a combination of DFT and non-equilibrium Green's function formalism (Fig. 2).

Initial STM $I(s)$ studies of the compounds **1a** ($(3.1 \pm 0.9) \times 10^{-5} \text{ G}_0$ or $2.4 \pm 0.7 \text{ nS}$) and **1b** ($(3.2 \pm 0.8) \times 10^{-5} \text{ G}_0$ or $2.5 \pm 0.6 \text{ nS}$) bearing solubilizing hexyloxy groups revealed essentially identical single-molecule conductance values, and hence little influence of the supporting phosphine ligands (**1a**, PPh_3 ; **1b**, PEt_3) on the conductance properties (Table 1, Fig. 3).⁴⁷ These values compare with that of the analogous organic compound $\text{Me}_3\text{SiC}\equiv\text{CC}_6\text{H}_4\text{C}\equiv\text{CC}_6\text{H}_4\text{C}\equiv\text{CC}_6\text{H}_4\text{C}\equiv\text{CSiMe}_3$ (**5**, $(2.75 \pm 0.55) \times 10^{-5} \text{ G}_0$ or $2.13 \pm 0.43 \text{ nS}$, Chart 1) of comparable molecular length (**1a** 2.12 nm; **1b** 2.05 nm; **5** 2.45 nm), also measured by the $I(s)$ method.⁹⁶ Break-off distances obtained from the $I(s)$ data from **1a** and **1b** are in reasonable agreement with these estimates of molecular length (Table 1).

The model junction constructed from **1a** contacted *via* the trimethylsilylethynyl moieties (Fig. 2) gave excellent agreement with the experimental results at $E_F - E_F^{\text{DFT}} = -0.4 \text{ eV}$ (Fig. 2).



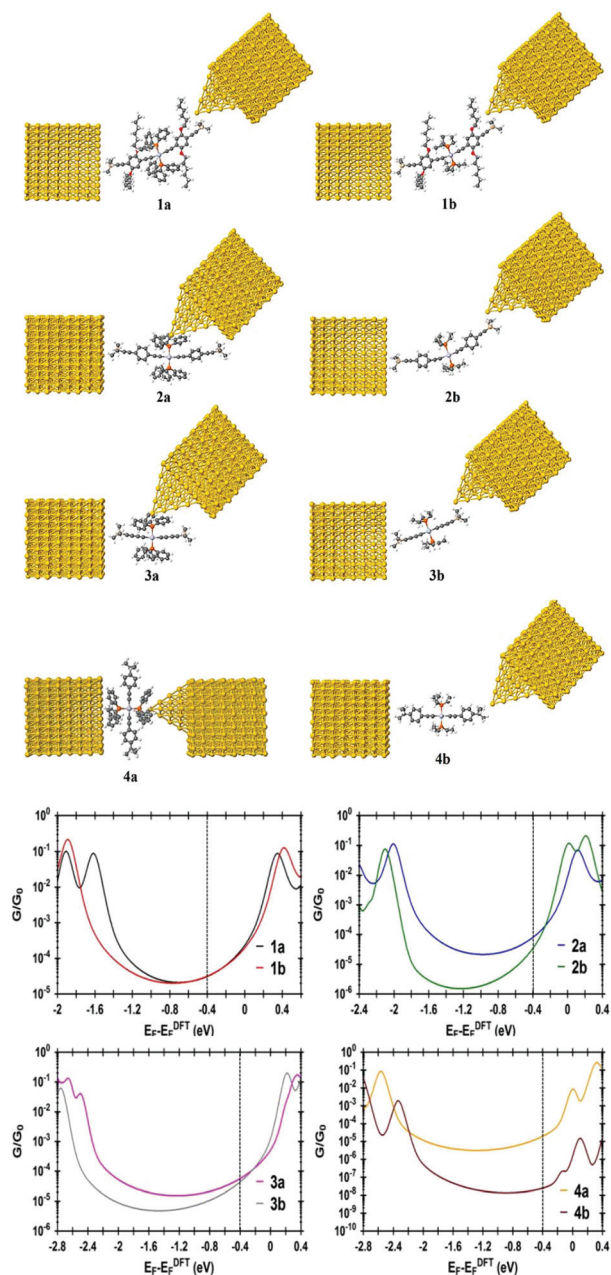


Fig. 2 The relaxed geometries from DFT model molecular junctions and plots showing selected comparisons of calculated conductance as a function of the Fermi energy for all molecular junctions. Black dashed lines show the chosen Fermi energy ($E_F = -0.4$ eV).

The tail of the molecular LUMO states aligns with this Fermi level (Fig. 2), indicating a charge transport mechanism involving tunnelling through the LUMO. A Mulliken Population Analysis of the frontier orbitals of **1a** and **1b** indicates that the energetically low-lying Pt orbitals make only a small contribution to the HOMO (**1a**, $\epsilon = -4.53$ eV, 7% Pt; **1b**, $\epsilon = -4.62$ eV, 8% Pt) and LUMO (**1a**, $\epsilon = -0.94$ eV, 8% Pt; **1b**, $\epsilon = -0.95$ eV, 8% Pt); instead these orbitals are largely diethynylbenzene in character (Fig. 4). Whilst the LUMO of **1b** is rather well separated from

another combination of the ligand π^* orbitals which forms LUMO+1 ($\epsilon = -0.72$ eV), for **1a** the LUMO+1 lies only some 0.02 eV higher in energy (at this level of theory) and is delocalised over the $\text{Ph}_3\text{P}-\text{Pt}-\text{PPh}_3$ fragment (Pt 14%, PPh_3 , 80%) (Fig. 4), and contributions from the PPh_3 ligands also dominate the next 14 unoccupied orbitals.

Schull and colleagues have previously reported studies of self-assembled films of the platinum complexes *trans*-Pt($\text{C}\equiv\text{CC}_6\text{H}_4\text{SAC})_2\text{L}_2$ ($\text{L} = \text{PCy}_3, \text{PBu}_3, \text{PPh}_3, \text{P}(\text{OEt})_3, \text{P}(\text{OPh})_3$) within crossed-wire molecular junctions.⁴⁷ Despite the modest (0.08 eV) variation in the HOMO-LUMO gap as a function of the supporting ligand, L , the I - V characteristics of these film-based junctions were also identical within experimental error. On the basis of these conductance results from both crossed-wire thin-films of Schull and those from *I*(s) single-molecule based junctions of **1a** and **1b** described here, it could initially be concluded that the supporting ligands L play no significant role in the electrical characteristics of the junctions formed from *trans*-Pt($\text{C}\equiv\text{CR})_2\text{L}_2$ complexes.

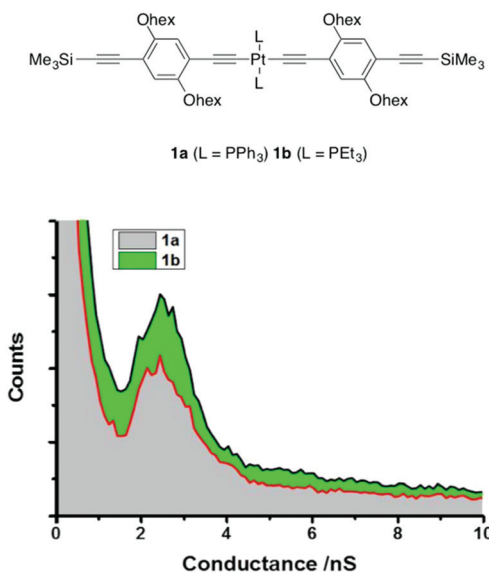
However, a more complex picture emerged when the study was extended to the complexes **2a**,**b** (Chart 1) of similar structure and comparable molecular length (Table 1). Solubilizing alkoxy groups, such as those present in **1a** and **1b**, play little role in tuning the conductance behavior of all-organic oligo(phenylene ethynylene)-based molecular wires,¹⁰² yet the conductance histogram of triphenylphosphine-supported **2a** revealed a much less pronounced peak, at significantly higher conductance ($(7.9 \pm 1.1) \times 10^{-5} G_0$ or 6.1 ± 0.85 nS) and a shorter break-off distance (1.70 ± 0.1 nm), than found for **1a** and **1b** (Table 1 and Fig. 5). However, the experimentally determined conductance of the triethylphosphine complex **2b** forms a more well-defined peak in the histogram ($(3.2 \pm 1.3) \times 10^{-5} G_0$ or 2.5 ± 1.0 nS) which is entirely in line with the values expected from **1a** and **1b**, and with better agreement between the experimental break-off distance (2.1 ± 0.15 nm) and the estimated Si...Si distance (2.40 nm) (Table 1 and Fig. 5). Computationally derived model junctions constructed for **2a** ($3.1 \times 10^{-5} G_0$ or 2.4 nS) (Table S1 and Fig. S9[†] (Model C)) and **2b** ($3.5 \times 10^{-5} G_0$ or 2.7 nS) (Table 1 and Fig. 2) with contact through the trimethylsilyl ethynyl moieties gave computed conductance values close to those expected, causing further consideration of the experimental result for **2a**.

As noted above, the trimethylsilyl ethynyl molecule-gold contact has been studied in a number of contexts,^{91–96} and is well described in terms of physisorption of the methyl groups, augmented by a degree of charge transfer when residing near to surface defects.^{14,67} It is only these latter situations that give rise to $\text{C}\equiv\text{CSiMe}_3$ -contacted junctions of sufficient conductance to be measured. However, the potential for molecules to bind in a number of distinct configurations within a molecular junction, each offering a distinct contact and hence conductance value, has been recognized. As phenyl rings are known to bind at defect sites to give rise to molecular junctions,^{64,103} and the PPh_3 ligands make a significant contribution to the low-lying unoccupied orbitals of **1a**, a second model junction was explored in which a molecule of **2a** is contacted by the

Table 1 Summary of the conductance values and geometries from experimental and computational molecular junctions

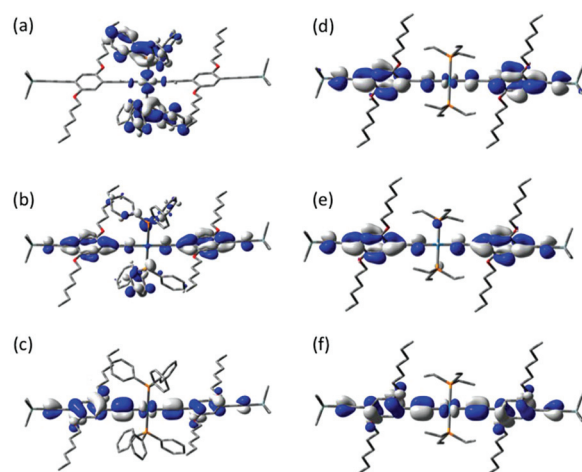
		Exp. G/G_0 ^a	Th. G/G_0 ^b	Z^* ^c (nm)	Z^d (nm)	Si...Si distance ^e (nm)	Anchor group
1a	<i>trans</i> -Pt{C≡CC ₆ H ₄ (Ohex) ₂ C≡CSiMe ₃ } ₂ (PPh ₃) ₂	$3.1 \pm 0.9 \times 10^{-5}$	3.1×10^{-5}	1.84 ± 0.1	2.11	2.39	C≡CSiMe ₃
1b	<i>trans</i> -Pt{C≡CC ₆ H ₄ (Ohex) ₂ C≡CSiMe ₃ } ₂ (PEt ₃) ₂	$3.2 \pm 0.8 \times 10^{-5}$	3.2×10^{-5}	2.05 ± 0.2	2.21	2.39	C≡CSiMe ₃
2a	<i>trans</i> -Pt{C≡CC ₆ H ₄ C≡CSiMe ₃ } ₂ (PPh ₃) ₂	$7.9 \pm 1.1 \times 10^{-5}$	8.0×10^{-5}	1.70 ± 0.1	1.73	2.40 ^g	PPh ₃
2b	<i>trans</i> -Pt{C≡CC ₆ H ₄ C≡CSiMe ₃ } ₂ (PEt ₃) ₂	$3.2 \pm 1.3 \times 10^{-5}$	3.5×10^{-5}	2.1 ± 0.15	2.31	2.40 ^g	C≡CSiMe ₃
3a	<i>trans</i> -Pt{C≡CC≡CSiMe ₃ } ₂ (PPh ₃) ₂	$5.2 \pm 1.6 \times 10^{-5}$	5.7×10^{-5}	1.38 ± 0.1	1.37	1.53	PPh ₃
3b	<i>trans</i> -Pt{C≡CC≡CSiMe ₃ } ₂ (PEt ₃) ₂	$4.9 \pm 1.0 \times 10^{-5}$	4.5×10^{-5}	1.70 ± 0.17	1.72	1.53	C≡CSiMe ₃
4a	<i>trans</i> -Pt{C≡CC ₆ H ₄ Bu ^t } ₂ (PPh ₃) ₂	$4.1 \pm 0.6 \times 10^{-5}$	1.98×10^{-5}	1.46 ± 0.21	1.05/1.40 ^f nm	PPh ₃	PPh ₃
4b	<i>trans</i> -Pt{C≡CC ₆ H ₄ Bu ^t } ₂ (PEt ₃) ₂	No peak	2.46×10^{-8}	—	2.23	—	—

^aThe experimental conductance determined from $I(s)$ measurements. ^bThe calculated conductance values G/G_0 at $E_F - E_F^{\text{DFT}} = -0.4$ eV from model junctions. ^cExperimental break-off distance from $I(s)$ measurements. ^dThe calculated electrode separation in a relaxed junction, $Z = d_{\text{Au-Au}} - 0.25$ nm, where 0.25 nm is the calculated center-to-center distance of the apex atoms of the two opposing gold electrodes when conductance = G_0 in the absence of a molecule. ^eSi...Si distance from DFT optimised gas-phase geometries. ^fSee Fig. S11. ^gCrystallographically determined distance 2.37 nm.

**Fig. 3** $I(s)$ conductance histograms of **1a** and **1b** constructed from 500 traces.

STM tip at one of the ostensibly ancillary PPh_3 ligands (Fig. 2 and Table 1). The calculated conductance of this alternative contact geometry ($8.0 \times 10^{-5} G_0$) is in excellent agreement with the experimental value ($(7.9 \pm 1.1) \times 10^{-5} G_0$ or 6.1 ± 0.85 nS). Moreover, a calculated break-off distance (1.73 nm) in agreement with experiment (1.70 ± 0.1 nm) was obtained (Table 1). A further model in which the junction is formed by contact across both *trans*-disposed PPh_3 ligand sets (Table S1 and Fig. S9,† Model B) gave a significantly higher calculated conductance ($3.44 \times 10^{-4} G_0$ or 26.6 nS) and a much shorter break-off distance (1.05 nm) than the experimental values (see also discussion below).

It is therefore quite probable that the peak observed in the conductance histogram of **2a** (Fig. 5) is derived from adventitious contact of the STM tip to one of the bulky PPh_3 ligands rather than to the 'designated' C≡CSiMe₃ contact. The flexible hexyloxy chains, initially introduced to improve the solubility

**Fig. 4** Plots of selected frontier orbitals of **1a** (a, LUMO+1; b, LUMO; c, HOMO) and **1b** (d, LUMO+1; e, LUMO; f, HOMO). In this and all other plots, iso-surfaces are shown at ± 0.03 (e per $\text{bohr}^{3/2}$).

of compounds **1a** and **1b**, therefore also appear to play a role in preventing the approach of the STM tip to the PPh_3 ligand, effectively 'insulating' the PPh_3 ligands from contacting to the electrodes. Similarly, the absence of any significant electron density on the alkyl chains of the PEt_3 ligands in the frontier orbitals of **1b** and **2b** ensures more conductive molecular junctions are formed by contacts between the electrodes and the trimethylsilyl ethynyl groups. Thus, for the identically-contacted compounds **1a**, **1b**, and **2b** the junction conductances are identical (Table 1), whilst the higher values measured for **2a** can be attributed to the binding of the molecule in the junction through one of the PPh_3 ligands (Fig. 2). Interestingly, molecular junctions formed with the bis(platinum) octatetrayndiyl complex $[\text{Pt}(\text{SAC})\{\text{P}(p\text{-tol})_3\}_2]_2(\mu\text{-C}\equiv\text{CC}\equiv\text{CC}\equiv\text{C})$ (*p*-tol = 4-MeC₆H₄⁻) by the mechanically controlled break junction (MCBJ) method were observed to be rather unstable, with broadening of peaks in the dI/dV plots ascribed to various instabilities in the junction including structural fluctuations.⁴⁹ Given the steric encum-



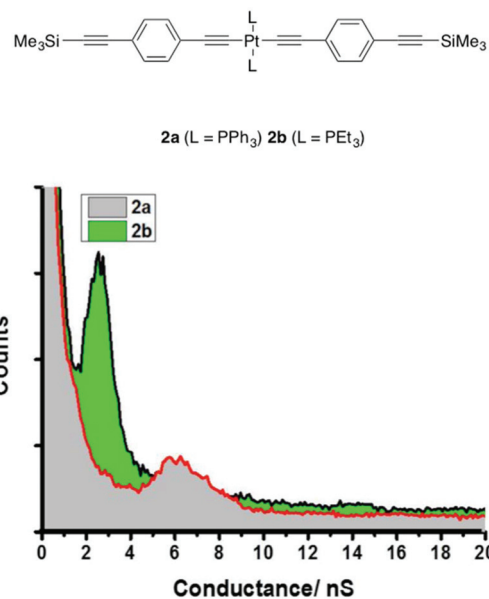


Fig. 5 $I(s)$ conductance histograms of **2a** and **2b** constructed from 500 traces.

brance around the thiolate group in this complex, adventitious contact through the tolyl moieties of the supporting phosphine ligands may now be suggested as a contributing factor to these junction instabilities and peak broadening.

The frontier orbitals of **2a** and **2b** were analyzed (Fig. 6) in part to explore if such junction geometries might be predicted from the molecular electronic structure, which, in turn, might aid future molecular design concepts. Whilst the HOMOs are also significantly diethynylbenzene in character, with a small contribution from the Pt atom, (**2a** HOMO Pt 8%; **2b** HOMO 11%), the LUMO of **2a** is now found to be largely PPh_3 in character (76%) and somewhat separated from the other frontier orbitals (ΔE HOMO-LUMO 3.92 eV; ΔE LUMO-(LUMO+1) 0.09

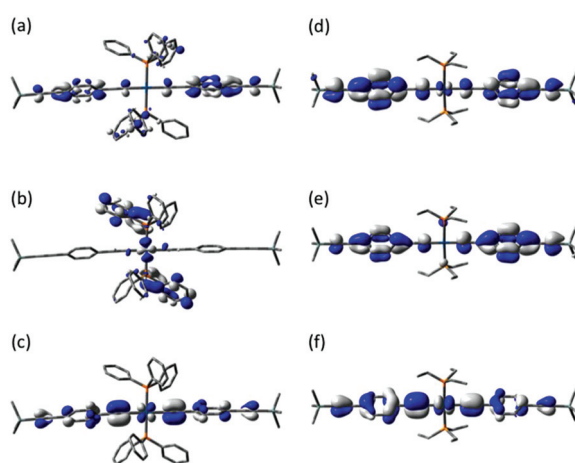


Fig. 6 Plots of selected frontier orbitals of **2a** (a, LUMO+1; b, LUMO; c, HOMO) and **2b** (d, LUMO+1; e, LUMO; f, HOMO).

eV). The LUMO and LUMO+1 of **2b** are both delocalized over the diethynylbenzene and Pt centre. Although the conductance channel cannot be predicted from simple inspection of MOs, the presence of the low-lying phosphine π^* orbitals is consistent with the results from the experimental and model junctions.

To explore this concept further, the electronic structures of the bis(diynyl) complexes *trans*-Pt(C≡CC≡CSiMe₃)₂(PPh₃)₂ (**3a**) and *trans*-Pt(C≡CC≡CSiMe₃)₂(PEt₃)₂ (**3b**) were also compared and the compounds examined in both experimental and computational molecular junctions. The HOMO of **3a** (-5.04 eV) and **3b** (-5.17 eV) are of similar energy and almost identically composed (Fig. 7). However, again the exchange of PPh₃ for PEt₃ has a significant influence on the energy and composition of the unoccupied frontier molecular orbitals. In the case of **3a** the PPh₃ ligands contribute almost exclusively to the LUMO (-1.09 eV) and the next 12 unoccupied orbitals. The LUMO+13 of **3a** (+0.16 eV), whilst featuring only a small contribution from the Pt center (2%), is the lowest lying orbital to be largely comprised of contributions from atoms within the diynyl ligands. In contrast, the LUMO of **3b** (-0.97 eV), which is well removed from the other frontier orbitals, is delocalized over the 11-atom Si-C₄-Pt-C₄-Si chain.

The single-molecule conductance measurements initially belie the influence of these differences in electronic structure on the characteristics of the junction, with both **3a** ($(5.2 \pm 1.6) \times 10^{-5} G_0$ or 4.0 ± 1.2 nS) and **3b** ($(4.9 \pm 1.0) \times 10^{-5} G_0$ or 3.8 ± 0.8 nS) giving rise to conductance histograms with peaks at similar conductance values (Fig. 8). However, the experimentally determined break-off distance is somewhat shorter for the PPh₃ ligated complex **3a** (1.38 ± 0.10 nm) than PEt₃ substituted **3b** (1.70 ± 0.17 nm), which compares with the Si···Si distance of 1.53 nm in each case (Table 1). From the model junction with two trimethylsilylthiethyl contacts (Fig. S9,† Model C), a calculated conductance value of $4.23 \times 10^{-5} G_0$ or 3.28 nS was obtained from **3a** (Fig. S10†), which although in

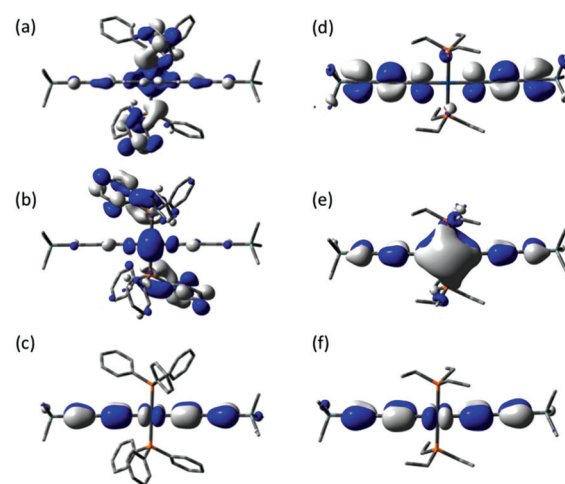
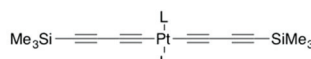
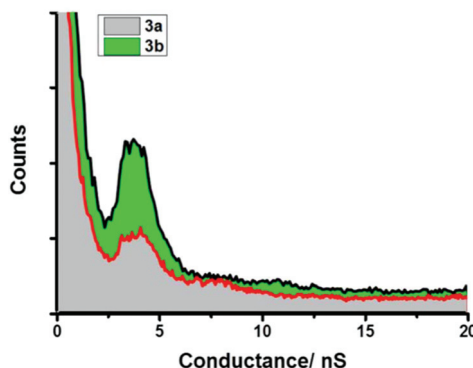
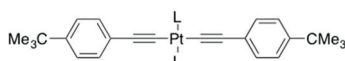
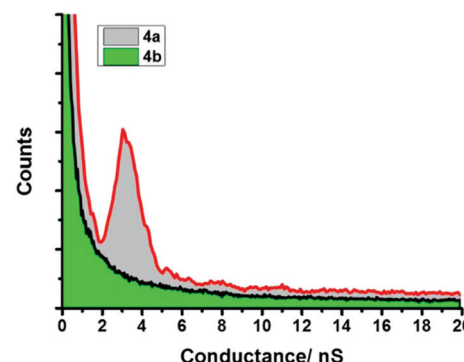


Fig. 7 Plots of selected frontier orbitals of **3a** (a, LUMO+1; b, LUMO; c, HOMO) and **3b** (d, LUMO+1; e, LUMO; f, HOMO).



3a (L = PPh₃) 3b (L = PEt₃)Fig. 8 $I(s)$ conductance histograms of 3a and 3b constructed from 500 traces.4a (L = PPh₃) 4b (L = PEt₃)Fig. 9 $I(s)$ conductance histograms of 4a and 4b constructed from 500 traces.

fairly good agreement with the experimental value, gave an estimated break-off distance of 1.72 nm, considerably longer than the experimental value.

As with 2a, a model junction of 3a with two triphenylphosphine contacts (Fig. S9,† Model B) gave a calculated conductance value of $5.66 \times 10^{-4} G_0$ or 7.22 nS (Fig. S10 and Table S1†) and an estimated break-off distance of 1.03 nm, in poor agreement with experiment ($G = 5.2 \pm 1.6 \times 10^{-5} G_0$ or 4.0 ± 1.2 nS; $Z^* = 1.38 \pm 0.1$ nm). However, a model junction in which the STM tip is allowed to contact one of the PPh₃ ligands in 3a (Fig. 2 and Fig. S9,† Model A) gave better overall agreement with a calculated conductance of $5.70 \times 10^{-5} G_0$ or 4.41 nS and break-off distance of 1.37 nm. The model junction constructed from trimethylsilylethynyl-contacted 3b (Fig. 2) gave good agreement between the experimental ($(4.9 \pm 1.0) \times 10^{-5} G_0$ or 3.8 ± 0.8 nS; break-off distance 1.70 ± 0.17 nm) and calculated ($4.50 \times 10^{-5} G_0$ or 3.49 nS; break-off distance 1.72 nm).

To conclusively demonstrate the significance of the PPh₃ contacts in these Pt-complex based molecular junctions, the model compounds *trans*-Pt(C≡CC₆H₄Bu')₂(PPh₃)₂ (**4a**) and *trans*-Pt(C≡CC₆H₄Bu')₂(PEt₃)₂ (**4b**) were studied (Fig. 9 and Table 1). The alkynyl ligands were chosen to model the electronic effects of the alkynyl ligands in **1a,b-3a,b**, with the *tert*-butyl substituent ('Bu) introduced to prevent adventitious junction formation to that phenyl ring.¹⁰³ The $I(s)$ studies of **4a** revealed a peak in the conductance histogram ($(4.1 \pm 0.6) \times 10^{-5} G_0$ or 3.17 ± 0.46 nS). The experimental break-off distance (1.46 ± 0.21 nm) compares poorly with the estimated separation of the quaternary carbons of the 'Bu groups of 1.81 nm, but is much more consistent with the dimensions across the aryl rings of the phosphine ligands (*ca.* 1.4 nm). Three computational model junctions were constructed from **4a**, contacted through either a *tert*-butyl group and one PPh₃ ligand

(Fig. S9,† Model A), both PPh₃ ligands (Fig. 2 and Fig. S9,† Model B) or both the *tert*-butyl moieties (Fig. S9,† Model C) were constructed (Table S1†). Only the bis(PPh₃)-contacted junction gave conductance value and break-off distance consistent with the experimental data (Fig. S9-S11†). In contrast, $I(s)$ studies of **4b** bearing the trialkyl phosphine PEt₃ revealed no traces containing the current plateaus characteristic of single-molecule junction formation (Fig. S8†).

The binding energies of **3a**, chosen as a representative example of the compounds in the series, in a phosphine-contacted model junction were calculated over a range of electrode separations to provide further support for the hypothesis of competing contacts to different regions of the molecule (Fig. S12 and Table S2†). The trimethylsilylethynyl-gold binding energy has been estimated to fall between -0.40 and -0.74 eV over a range of gold-surface features.⁶⁷ As the phosphine-contacted junction is evolved to simulate the pulling of the junction, the binding energy naturally decreases from -3.46 eV to -0.12 eV (Table S2†). It is therefore likely that $I(s)$ junctions formed as the STM tip approaches and withdraws from the surface involve at least one PPh₃-based contact. Although bis(PPh₃)-contacted junctions (Fig. S9,† Model B), are energetically favorable at the shortest electrode separations (Table S2†), the formation of these junctions are likely geometrically limited by the closest tip-substrate approach distance in the $I(s)$ measurements (>1 nm) and the dimensions of the prolate-shaped molecules (Fig. S11†).

Finally, the conductance behavior of these platinum complexes in comparison with closely related organic compounds measured under similar conditions is deserving of comment. The electrical properties and conductance behavior of oligo(phenylene ethynylene)^{102,104-108} and oligo(yne) derivatives^{14,69,109,110} have been explored extensively. The oligo(phenylene ethynylene) compound $\text{Me}_3\text{SiC}\equiv\text{CC}_6\text{H}_4\text{C}\equiv\text{CC}_6\text{H}_4\text{C}\equiv\text{CC}_6\text{H}_4\text{C}\equiv\text{CSiMe}_3$ (**5**)



has an estimated Si...Si distance of 2.69 nm, and gives rise to a conductance value of $(2.75 \pm 0.56) \times 10^{-5} G_0$ or 2.13 ± 0.43 nS.⁹⁶ The trimethylsilylethynyl-contacted platinum complexes **1a**, bearing the insulating hexyloxy side chains, **1b** and **2b** offer comparable molecular lengths (2.39–2.40 nm) and similar conductances (Table 1). Clearly, the platinum center cannot be considered an insulating fragment *per se*, but in the present series is comparable in effect to the central phenylene ring in $\text{Me}_3\text{SiC}\equiv\text{CC}_6\text{H}_4\text{C}\equiv\text{CC}_6\text{H}_4\text{C}\equiv\text{CC}_6\text{H}_4\text{C}\equiv\text{CSiMe}_3$ (5).

For the trimethylsilylethynyl-contacted bis(diynyl) complex **3b** ($(4.9 \pm 1.0) \times 10^{-5} G_0$ or 3.8 ± 0.8 nS, Si...Si distance 1.53 nm) the observed conductance of the molecular junction may be compared with those reported earlier for the organic oligoynes $\text{Me}_3\text{SiC}\equiv\text{CC}\equiv\text{CSiMe}_3$ ($2.01 \times 10^{-5} G_0$ or 1.56 nS, Si...Si distance 0.76 nm), $\text{Me}_3\text{SiC}\equiv\text{CC}\equiv\text{CC}\equiv\text{CSiMe}_3$ ($1.63 \times 10^{-5} G_0$ or 1.26 nS, Si...Si distance 1.06 nm), $\text{Me}_3\text{SiC}\equiv\text{CC}\equiv\text{CC}\equiv\text{CC}\equiv\text{CSiMe}_3$ ($1.42 \times 10^{-5} G_0$ or 1.10 nS, Si...Si distance 1.33 nm) and $\text{Me}_3\text{SiC}\equiv\text{CC}\equiv\text{CC}\equiv\text{CC}\equiv\text{CSiMe}_3$ ($0.90 \times 10^{-5} G_0$ or 0.70 nS, Si...Si distance 1.60 nm) in the same solvent.¹⁴ The relative values of conductance obtained from **3b** and the octatrayne indicate that introduction of the *trans*-Pt(PEt₃)₂ fragment within the oligoyne chain gives rise to molecules of greater conductance than those prepared by homo-coupling through a carbon–carbon sigma bond, or insertion of another alkyne –C≡C– moiety. We can, therefore, conclude that although the platinum center makes little contribution to the LUMO, there is no detrimental effect on the conductance of these molecules with LUMO-based conduction channels. Similar concepts have been proposed to account for the high conductance of Cr₃-metal strings despite the absence of extensively delocalized frontier orbitals.^{54,55}

Conclusion

The d⁸ square-planar platinum complexes **1a** ($(3.1 \pm 0.9) \times 10^{-5} G_0$), **1b** ($(3.2 \pm 0.8) \times 10^{-5} G_0$), **2b** ($(3.2 \pm 1.3) \times 10^{-5} G_0$) and **3b** ($(4.9 \pm 1.0) \times 10^{-5} G_0$) form molecular junctions in *I*(*s*) experiments with conductance commensurate with similarly structured all-organic oligo(phenylene ethynylene) and oligoyne compounds. The PPh₃ supporting ligands in the series **2a–4a** provide an alternative contact point in the molecular junctions, although the introduction of solubilising hexyloxy side chains to the diethynylbenzene ligands in **1a** hinders this contact and effectively insulates these alternative contact points. Thus, despite the wide-spread use of PPh₃ and other aryl-phosphines as ancillary ligands in organometallic chemistry, these moieties can clearly have unintended consequences for single-molecule conductance measurements arising from adventitious contacts and formation of un-anticipated molecular junctions. The hexyloxy groups in **1a** serve to effectively insulate these alternate contacts. Otherwise, the use of trialkyl-phosphines, such as PEt₃ here, is effective in both maintaining sufficient compound solubility and preventing adventitious junction formation through the ancillary ligands. It is also

important to note the simplicity with which *trans*-bis(alkynyl) platinum(II) complexes can be synthesized. These results provide a considerable body of information concerning the design of organometallic complexes for use in molecular electronics.

Acknowledgements

C. J. L. and O. A. A. acknowledge financial support from the Ministry of Higher Education and Scientific Research of Iraq. C. J. L. and M. R. B. acknowledges funding from the EU through the FP7 ITN MOLESCO (project number 212942). M. R. B. thanks the EPSRC for funding (grant EP/K039423/1). P. J. L. holds an ARC Future Fellowship (FT120100073) and gratefully acknowledges funding for this work from the ARC (DP140100855, LE150100148). S. B. holds an International Postgraduate Research Scholarship and gratefully acknowledges support from the University of Western Australia. R. J. N. and S. J. H. thank EPSRC for funding (grant EP/H035184/1 and EP/K007785/1). M. S. I., N. J. L. and T. A. acknowledge the Leverhulme Trust (RPG 2012-754) for funding. M. S. I. is supported by a Marie Skłodowska Curie Global Fellowship (MOLCLICK: 657247) within the Horizon 2020 Programme.

Notes and references

- 1 R. J. Nichols, W. Haiss, S. J. Higgins, E. Leary, S. Martín and D. Bethell, *Phys. Chem. Chem. Phys.*, 2010, **12**, 2801–2815.
- 2 R. M. Metzger, *Chem. Rev.*, 2015, **115**, 5056–5115.
- 3 S. G. Lemay, S. Kang, K. Mathwig and P. S. Singh, *Acc. Chem. Res.*, 2013, **46**, 369–377.
- 4 C. Li, A. Mishchenko and T. Wandlowski, in *Unimolecular and Supramolecular Electronics II*, Springer, Berlin, Heidelberg, 2011, vol. 313, pp. 121–188.
- 5 D. Xiang, X. Wang, C. Jia, T. Lee and X. Guo, *Chem. Rev.*, 2016, **116**, 4318–4440.
- 6 L. Sun, Y. A. Diaz-Fernandez, T. A. Gschneidtner, F. Westerlund, S. Lara-Avila and K. Moth-Poulsen, *Chem. Soc. Rev.*, 2014, **43**, 7378–7411.
- 7 W. Sheng, Z. Y. Li, Z. Y. Ning, Z. H. Zhang, Z. Q. Yang and H. Guo, *J. Chem. Phys.*, 2009, **131**, 244712.
- 8 W. Haiss, H. Van Zalinge, D. Bethell, J. Ulstrup, D. J. Schiffrian and R. J. Nichols, *Faraday Discuss.*, 2006, **131**, 253–264.
- 9 C. Li, I. Pobelov, T. Wandlowski, A. Bagrets, A. Arnold and F. Evers, *J. Am. Chem. Soc.*, 2008, **130**, 318–326.
- 10 V. Fatemi, M. Kamenetska, J. B. Neaton and L. Venkataraman, *Nano Lett.*, 2011, **11**, 1988–1992.
- 11 B. Capozzi, J. Xia, O. Adak, E. J. Dell, Z. F. Liu, J. C. Taylor, J. B. Neaton, L. M. Campos and L. Venkataraman, *Nat. Nanotechnol.*, 2015, **10**, 522–527.



12 M. Kotiuga, P. Darancet, C. R. Arroyo, L. Venkataraman and J. B. Neaton, *Nano Lett.*, 2015, **15**, 4498–4503.

13 B. Choi, B. Capozzi, S. Ahn, A. Turkiewicz, G. Lovat, C. Nuckolls, M. L. Steigerwald, L. Venkataraman and X. Roy, *Chem. Sci.*, 2016, **7**, 2701–2705.

14 D. C. Milan, O. A. Al-Owaedi, M. C. Oerthel, S. Marqués-González, R. J. Brooke, M. R. Bryce, P. Cea, J. Ferrer, S. J. Higgins, C. J. Lambert, P. J. Low, D. Z. Manrique, S. Martín, R. J. Nichols, W. Schwarzacher and V. M. García-Suárez, *J. Phys. Chem. C*, 2016, **120**, 15666–15674.

15 N. J. Kay, S. J. Higgins, J. O. Jeppesen, E. Leary, J. Lycoops, J. Ulstrup and R. J. Nichols, *J. Am. Chem. Soc.*, 2012, **134**, 16817–16826.

16 H. M. Osorio, S. Catarelli, P. Cea, J. B. G. Gluyas, F. Hartl, S. J. Higgins, E. Leary, P. J. Low, S. Martín, R. J. Nichols, J. Tory, J. Ulstrup, A. Vezzoli, D. C. Milan and Q. Zeng, *J. Am. Chem. Soc.*, 2015, **137**, 14319–14328.

17 A. Vezzoli, I. Grace, C. Brooke, K. Wang, C. J. Lambert, B. Xu, R. J. Nichols and S. J. Higgins, *Nanoscale*, 2015, **7**, 18949–18955.

18 C. Huang, A. V. Rudnev, W. Hong and T. Wandlowski, *Chem. Soc. Rev.*, 2015, **44**, 889–901.

19 M. Baghernejad, X. Zhao, K. Baruël Ørnsø, M. Füeg, P. Moreno-García, A. V. Rudnev, V. Kaliginedi, S. Vesztergom, C. Huang, W. Hong, P. Broekmann, T. Wandlowski, K. S. Thygesen and M. R. Bryce, *J. Am. Chem. Soc.*, 2014, **136**, 17922–17925.

20 Z. Li, H. Li, S. Chen, T. Froehlich, C. Yi, C. Schönenberger, M. Calame, S. Decurtins, S. X. Liu and E. Borguet, *J. Am. Chem. Soc.*, 2014, **136**, 8867–8870.

21 P. J. Low, *Dalton Trans.*, 2005, 2821–2824.

22 S. Rigaut, *Dalton Trans.*, 2013, **42**, 15859–15863.

23 T. Ren, *Organometallics*, 2005, **24**, 4854–4870.

24 J. Ponce, C. R. Arroyo, S. Tatay, R. Frisenda, P. Gaviña, D. Aravena, E. Ruiz, H. S. J. van der Zant and E. Coronado, *J. Am. Chem. Soc.*, 2014, **136**, 8314–8322.

25 E. A. Osorio, K. Moth-Poulsen, H. S. J. van der Zant, J. Paaske, P. Hedegård, K. Flensberg, J. Bendix and T. Bjørnholm, *Nano Lett.*, 2010, **10**, 105–110.

26 F. Schwarz, G. Kastlunger, F. Lissel, C. Egler-Lucas, S. N. Semenov, K. Venkatesan, H. Berke, R. Stadler and E. Lörtscher, *Nat. Nanotechnol.*, 2016, **11**, 170–176.

27 S. A. Hua, M. C. Cheng, C. H. Chen and S. M. Peng, *Chem. Ber.*, 2015, **2015**, 2510–2523.

28 X. Roy, C. L. Schenck, S. Ahn, R. A. Lalancette, L. Venkataraman, C. Nuckolls and M. L. Steigerwald, *Angew. Chem., Int. Ed.*, 2012, **51**, 12473–12476.

29 E. Leary, H. Van Zalinge, S. J. Higgins, R. J. Nichols, F. Fabrizi De Biani, P. Leoni, L. Marchetti and P. Zanello, *Phys. Chem. Chem. Phys.*, 2009, **11**, 5198–5202.

30 T. Tanaka and A. Osuka, *Chem. Soc. Rev.*, 2015, **44**, 943–969.

31 M. Jurow, A. E. Schuckman, J. D. Batteas and C. M. Drain, *Coord. Chem. Rev.*, 2010, **254**, 2297–2310.

32 S. A. Getty, C. Engtrakul, L. Wang, R. Liu, S. H. Ke, H. U. Baranger, W. Yang, M. S. Fuhrer and L. R. Sita, *Phys. Rev. B: Condens. Matter*, 2005, **71**, 241401.

33 Y. Y. Sun, Z. L. Peng, R. Hou, J.-H. Liang, J. F. Zheng, X. Y. Zhou, X. S. Zhou, S. Jin, Z. J. Niu and B.-W. Mao, *Phys. Chem. Chem. Phys.*, 2014, **16**, 2260–2267.

34 T. Albrecht, A. Guckian, A. M. Kuznetsov, J. G. Vos and J. Ulstrup, *J. Am. Chem. Soc.*, 2006, **128**, 17132–17138.

35 T. Albrecht, K. Moth-Poulsen, J. B. Christensen, A. Guckian, T. Bjørnholm, J. G. Vos and J. Ulstrup, *Faraday Discuss.*, 2006, **131**, 265–279.

36 T. Albrecht, A. Guckian, J. Ulstrup and J. G. Vos, *Nano Lett.*, 2005, **5**, 1451–1455.

37 R. Sakamoto, S. Katagiri, H. Maeda and H. Nishihara, *Coord. Chem. Rev.*, 2013, **257**, 1493–1506.

38 B. Kim, J. M. Beebe, C. Olivier, S. Rigaut, D. Touchard, J. G. Kushmerick, X. Y. Zhu and C. D. Frisbie, *J. Phys. Chem. C*, 2007, **111**, 7521–7526.

39 L. Luo, A. Benameur, P. Brignou, S. H. Choi, S. Rigaut and C. D. Frisbie, *J. Phys. Chem. C*, 2011, **115**, 19955–19961.

40 A. Mulas, Y. M. Hervault, L. Norel, S. Rigaut and C. Lagrost, *ChemElectroChem*, 2015, **2**, 1799–1805.

41 A. Mulas, Y. M. Hervault, X. He, E. Di Piazza, L. Norel, S. Rigaut and C. Lagrost, *Langmuir*, 2015, **31**, 7138–7147.

42 F. Meng, Y. M. Hervault, Q. Shao, B. Hu, L. Norel, S. Rigaut and X. Chen, *Nat. Commun.*, 2014, **5**, 3023.

43 F. Meng, Y. M. Hervault, L. Norel, K. Costuas, C. Van Dyck, V. Geskin, J. Cornil, H. H. Hng, S. Rigaut and X. Chen, *Chem. Sci.*, 2012, **3**, 3113–3118.

44 F. Lissel, F. Schwarz, O. Blacque, H. Riel, E. Lörtscher, K. Venkatesan and H. Berke, *J. Am. Chem. Soc.*, 2014, **136**, 14560–14569.

45 F. Schwarz, G. Kastlunger, F. Lissel, H. Riel, K. Venkatesan, H. Berke, R. Stadler and E. Lörtscher, *Nano Lett.*, 2014, **14**, 5932–5940.

46 K. Liu, X. Wang and F. Wang, *ACS Nano*, 2008, **2**, 2315–2323.

47 T. L. Schull, J. G. Kushmerick, C. H. Patterson, C. George, M. H. Moore, S. K. Pollack and R. Shashidhar, *J. Am. Chem. Soc.*, 2003, **125**, 3202–3203.

48 M. Mayor, C. Von Hänisch, H. B. Weber, J. Reichert and D. Beckmann, *Angew. Chem., Int. Ed.*, 2002, **41**, 1183–1186.

49 S. Ballmann, W. Hieringer, D. Secker, Q. Zheng, J. A. Gladysz, A. Görling and H. B. Weber, *ChemPhysChem*, 2010, **11**, 2256–2260.

50 G. Frapper and M. Kertesz, *Inorg. Chem.*, 1993, **32**, 732–740.

51 M. Parthey, K. B. Vincent, M. Renz, P. A. Schauer, D. S. Yufit, J. A. K. Howard, M. Kaupp and P. J. Low, *Inorg. Chem.*, 2014, **53**, 1544–1554.

52 S. Marqués-González, M. Parthey, D. S. Yufit, J. A. K. Howard, M. Kaupp and P. J. Low, *Organometallics*, 2014, **33**, 4947–4963.

53 P. J. West, M. P. Cifuentes, T. Schwich, M. D. Randles, J. P. Morrall, E. Kulasekera, S. Petrie, R. Stranger and M. G. Humphrey, *Inorg. Chem.*, 2012, **51**, 10495–10502.



54 V. P. Georgiev and J. E. McGrady, *J. Am. Chem. Soc.*, 2011, **133**, 12590–12599.

55 V. P. Georgiev, P. J. Mohan, D. DeBrincat and J. E. McGrady, *Coord. Chem. Rev.*, 2013, **257**, 290–298.

56 O. A. Al-Owaedi, D. C. Milan, M. C. Oerthel, S. Bock, D. S. Yufit, J. A. K. Howard, S. J. Higgins, R. J. Nichols, C. J. Lambert, M. R. Bryce and P. J. Low, *Organometallics*, 2016, **35**, 2944–2954.

57 M. G. Reuter, T. Seideman and M. A. Ratner, *J. Chem. Phys.*, 2011, **134**, 154708.

58 R. Frisenda, S. Tarkuç, E. Galán, M. L. Perrin, R. Eelkema, F. C. Grozema and H. S. J. van der Zant, *Beilstein J. Nanotechnol.*, 2015, **6**, 1558–1567.

59 J. Hihath and N. Tao, *Semicond. Sci. Technol.*, 2014, **29**, 054007.

60 C. Jia and X. Guo, *Chem. Soc. Rev.*, 2013, **42**, 5642–5660.

61 S. Y. Quek, M. Kamenetska, M. L. Steigerwald, H. J. Choi, S. G. Louie, M. S. Hybertsen, J. B. Neaton and L. Venkataraman, *Nat. Nanotechnol.*, 2009, **4**, 230–234.

62 T. A. Su, J. R. Widawsky, H. Li, R. S. Klausen, J. L. Leighton, M. L. Steigerwald, L. Venkataraman and C. Nuckolls, *J. Am. Chem. Soc.*, 2013, **135**, 18331–18334.

63 V. Kaliginedi, A. V. Rudnev, P. Moreno-García, M. Baghernejad, C. Huang, W. Hong and T. Wandlowski, *Phys. Chem. Chem. Phys.*, 2014, **16**, 23529–23539.

64 W. Haiss, S. Martín, E. Leary, H. Van Zalinge, S. J. Higgins, L. Bouffier and R. J. Nichols, *J. Phys. Chem. C*, 2009, **113**, 5823–5833.

65 Z. L. Cheng, R. Skouta, H. Vazquez, J. R. Widawsky, S. Schneebeli, W. Chen, M. S. Hybertsen, R. Breslow and L. Venkataraman, *Nat. Nanotechnol.*, 2011, **6**, 353–357.

66 Y. Fu, S. Chen, A. Kuzume, A. Rudnev, C. Huang, V. Kaliginedi, M. Baghernejad, W. Hong, T. Wandlowski, S. Decurtins and S. X. Liu, *Nat. Commun.*, 2015, **6**, 6403.

67 R. R. Ferradás, S. Marqués-González, H. M. Osorio, J. Ferrer, P. Cea, D. C. Milan, A. Vezzoli, S. J. Higgins, R. J. Nichols, P. J. Low, V. M. García-Suárez and S. Martín, *RSC Adv.*, 2016, **6**, 75111–75121.

68 J. S. Meisner, M. Kamenetska, M. Krikorian, M. L. Steigerwald, L. Venkataraman and C. Nuckolls, *Nano Lett.*, 2011, **11**, 1575–1579.

69 P. Moreno-García, M. Gulcur, D. Z. Manrique, T. Pope, W. Hong, V. Kaliginedi, C. Huang, A. S. Batsanov, M. R. Bryce, C. Lambert and T. Wandlowski, *J. Am. Chem. Soc.*, 2013, **135**, 12228–12240.

70 L. Xiang, T. Hines, J. L. Palma, X. Lu, V. Mujica, M. A. Ratner, G. Zhou and N. Tao, *J. Am. Chem. Soc.*, 2016, **138**, 679–687.

71 S. T. Schneebeli, M. Kamenetska, Z. Cheng, R. Skouta, R. A. Friesner, L. Venkataraman and R. Breslow, *J. Am. Chem. Soc.*, 2011, **133**, 2136–2139.

72 C. Pan, C. Zhao, M. Takeuchi and K. Sugiyasu, *Chem. – Asian J.*, 2015, **10**, 1820–1835.

73 H. Masai, J. Terao and Y. Tsuji, *Tetrahedron Lett.*, 2014, **55**, 4035–4043.

74 J. Stahl, J. C. Bohling, E. B. Bauer, T. B. Peters, W. Mohr, J. M. Martín-Alvarez, F. Hampel and J. A. Gladysz, *Angew. Chem., Int. Ed.*, 2002, **41**, 1871–1876.

75 J. Stahl, W. Mohr, L. de Quadras, T. B. Peters, J. C. Bohling, J. M. Martín-Alvarez, G. R. Owen, F. Hampel and J. A. Gladysz, *J. Am. Chem. Soc.*, 2007, **129**, 8282–8295.

76 L. de Quadras, E. B. Bauer, J. Stahl, F. Zhuravlev, F. Hampel and J. A. Gladysz, *New J. Chem.*, 2007, **31**, 1594–1604.

77 G. R. Owen, S. Gauthier, N. Weisbach, F. Hampel, N. Bhuvanesh and J. A. Gladysz, *Dalton Trans.*, 2010, **39**, 5260–5271.

78 L. de Quadras, E. B. Bauer, W. Mohr, J. C. Bohling, T. B. Peters, J. M. Martín-Alvarez, F. Hampel and J. A. Gladysz, *J. Am. Chem. Soc.*, 2007, **129**, 8296–8309.

79 G. R. Owen, J. Stahl, F. Hampel and J. A. Gladysz, *Organometallics*, 2004, **23**, 5889–5892.

80 M. C. Clough, T. Fiedler, N. Bhuvanesh and J. A. Gladysz, *J. Organomet. Chem.*, 2016, **812**, 34–42.

81 L. D. Movsisyan, M. Franz, F. Hampel, A. L. Thompson, R. R. Tykwiński and H. L. Anderson, *J. Am. Chem. Soc.*, 2016, **138**, 1366–1376.

82 L. D. Movsisyan, D. V. Kondratuk, M. Franz, A. L. Thompson, R. R. Tykwiński and H. L. Anderson, *Org. Lett.*, 2012, **14**, 3424–3426.

83 H. Sahnoune, Z. Baranová, N. Bhuvanesh, J. A. Gladysz and J.-F. Halet, *Organometallics*, 2013, **32**, 6360–6367.

84 N. Weisbach, Z. Baranová, S. Gauthier, J. H. Reibenspies and J. A. Gladysz, *Chem. Commun.*, 2012, **48**, 7562–7564.

85 J. Terao, T. Hosomi, H. Masai, W. Matsuda, S. Seki, T. Fujihara and Y. Tsuji, *Chem. Lett.*, 2014, **43**, 1289–1291.

86 J. Terao, K. Homma, Y. Konoshima, R. Imoto, H. Masai, W. Matsuda, S. Seki, T. Fujihara and Y. Tsuji, *Chem. Commun.*, 2014, **50**, 658–660.

87 J. Terao, H. Masai, T. Fujihara and Y. Tsuji, *Chem. Lett.*, 2012, **41**, 652–653.

88 T. Hosomi, H. Masai, W. Matsuda, S. Seki, T. Fujihara, Y. Tsuji and J. Terao, *Chem. Lett.*, 2016, **45**, 931–933.

89 H. Masai, J. Terao, S. Seki, S. Nakashima, M. Kiguchi, K. Okoshi, T. Fujihara and Y. Tsuji, *J. Am. Chem. Soc.*, 2014, **136**, 1742–1745.

90 M. Kiguchi, S. Nakashima, T. Tada, S. Watanabe, S. Tsuda, Y. Tsuji and J. Terao, *Small*, 2012, **8**, 726–730.

91 N. Katsonis, A. Marchenko, S. Taillemite, D. Fichou, G. Chouraqui, C. Aubert and M. Malacria, *Chem. – Eur. J.*, 2003, **9**, 2574–2581.

92 N. Katsonis, A. Marchenko, D. Fichou and N. Barrett, *Surf. Sci.*, 2008, **602**, 9–16.

93 A. Nion, N. Katsonis, A. Marchenko, C. Aubert and D. Fichou, *New J. Chem.*, 2013, **37**, 2261–2265.

94 A. Marchenko, N. Katsonis, D. Fichou, C. Aubert and M. Malacria, *J. Am. Chem. Soc.*, 2002, **124**, 9998–9999.

95 G. Pera, S. Martín, L. M. Ballesteros, A. J. Hope, P. J. Low, R. J. Nichols and P. Cea, *Chem. – Eur. J.*, 2010, **16**, 13398–13405.

96 S. Marqués-González, D. S. Yufit, J. A. K. Howard, S. Martín, H. M. Osorio, V. M. García-Suárez, R. J. Nichols,



S. J. Higgins, P. Cea and P. J. Low, *Dalton Trans.*, 2013, **42**, 338–341.

97 D. Millar, L. Venkataraman and L. H. Doerrer, *J. Phys. Chem. C*, 2007, **111**, 17635–17639.

98 J. C. Bailar and H. Itatani, *Inorg. Chem.*, 1965, **4**, 1618–1620.

99 G. W. Parshall, *Inorg. Synth.*, 1970, **12**, 26–33.

100 K. Sonogashira, T. Yatake, Y. Tohda, S. Takahashi and N. Hagihara, *J. Chem. Soc., Chem. Commun.*, 1977, 291–292.

101 W. Haiss, H. Van Zalinge, S. J. Higgins, D. Bethell, H. Höbenreich, D. J. Schiffrin and R. J. Nichols, *J. Am. Chem. Soc.*, 2003, **125**, 15294–15295.

102 R. Huber, M. T. González, S. Wu, M. Langer, S. Grunder, V. Horhoiu, M. Mayor, M. R. Bryce, C. Wang, R. Jitchati, C. Schönenberger and M. Calame, *J. Am. Chem. Soc.*, 2008, **130**, 1080–1084.

103 S. Martín, I. Grace, M. R. Bryce, C. Wang, R. Jitchati, A. S. Batsanov, S. J. Higgins, C. J. Lambert and R. J. Nichols, *J. Am. Chem. Soc.*, 2010, **132**, 9157–9164.

104 J. M. Tour, *Acc. Chem. Res.*, 2000, **33**, 791–804.

105 X. Xiao, L. A. Nagahara, A. M. Rawlett and N. Tao, *J. Am. Chem. Soc.*, 2005, **127**, 9235–9240.

106 L. T. Cai, H. Skulason, J. G. Kushmerick, S. K. Pollack, J. Naciri, R. Shashidhar, D. L. Allara, T. E. Mallouk and T. S. Mayer, *J. Phys. Chem. B*, 2004, **108**, 2827–2832.

107 Q. Lu, K. Liu, H. Zhang, Z. Du, X. Wang and F. Wang, *ACS Nano*, 2009, **3**, 3861–3868.

108 V. Kaliginedi, P. Moreno-García, H. Valkenier, W. Hong, V. M. García-Suárez, P. Buiter, J. L. H. Otten, J. C. Hummelen, C. J. Lambert and T. Wandlowski, *J. Am. Chem. Soc.*, 2012, **134**, 5262–5275.

109 C. Wang, A. S. Batsanov, M. R. Bryce, S. Martín, R. J. Nichols, S. J. Higgins, V. M. García-Suárez and C. J. Lambert, *J. Am. Chem. Soc.*, 2009, **131**, 15647–15654.

110 S. Ballmann, W. Hieringer, R. Härtle, P. B. Coto, M. R. Bryce, A. Görling, M. Thoss and H. B. Weber, *Phys. Status Solidi B*, 2013, **250**, 2452–2457.

